# Geometric ordering, surface chemistry, band bending, and work function at decapped GaAs(100) surfaces

I. M. Vitomirov, A. Raisanen, A. C. Finnefrock, R. E. Viturro, and L. J. Brillson
*Xerox Webster Research Center, Webster, New York 14580*

P. D. Kirchner, G. D. Pettit, and J. M. Woodall
*IBM Thomas J. Watson Research Center, Yorktown Heights, New York 10598*
(Received 27 April 1992; revised manuscript received 7 August 1992)

We present a comprehensive study of epitaxially grown and As-coated GaAs(100) surfaces as a function of As desorption temperature and background pressure. We have used low-energy electron diffraction to determine surface reconstruction, and core-level and valence-band soft-x-ray photoemission spectroscopy to perform chemical and electronic characterization of these surfaces. We find gradual changes in surface geometry and composition, and a limited ($\sim 120$ meV) Fermi-level movement over numerous reconstructions in the 250–650 °C annealing temperature range. The surface ionization potential and work function exhibit large changes between different surface reconstructions. In conjunction with other techniques, work-function measurements present evidence of surface inhomogeneity for many of the desorption temperatures and surface reconstructions. This inhomogeneity appears related to the existence of differently reconstructed patches on the surface. Our results emphasize the complexity of reconstructed GaAs(100) surfaces and the advantages of a multiple-technique approach for their characterization.

## I. INTRODUCTION

The (100) surface of GaAs exhibits a variety of scientifically and technologically relevant properties. Because of the polar nature and the related variety of reconstructions of this surface, its physical properties are significantly affected by its atomic composition.[1–7] The As-rich $(2\times4)$-$c(2\times8)$ and $c(4\times4)$ reconstructions and the Ga-rich $(4\times2)$-$c(8\times2)$ and $(4\times6)$ reconstructions have been intensely studied from both the experimental and theoretical points of view.[8–12] In addition, the more Ga-rich surfaces with the $(4\times2)$-$c(8\times2)$ reconstruction have attracted significant attention as a test bed for studies of Schottky barrier evolution at metal/GaAs interfaces.[5,13,14] Pioneering studies at As-encapsulated surfaces prepared by molecular-beam epitaxy (MBE) under less well-defined surface conditions suggested increased sensitivity of the interface Fermi-level ($E_F$) position to the particular metal overlayer, as compared to the "universal $E_F$ pinning" at the GaAs(110) surface.[15–17] However, with additional studies it has become increasingly apparent that the metal-semiconductor interface electronic properties, as well as the surface characteristics of GaAs(100), depend sensitively on details of surface preparation.[18–20]

The purpose of this paper is to explore the correlation of geometric, chemical, and electronic properties of decapped MBE-grown GaAs(110) surfaces. We have used core-level and valence-band soft-x-ray photoemission spectroscopy (SXPS) to study *in vacuo* surface chemistry, $E_F$ movement, and work-function changes over the full range (250–650 °C) of As desorption temperatures and subject to controlled variations of As background pressure. These experiments were combined with low-energy electron-diffraction (LEED) studies of thermally and chemically induced changes in surface reconstruction.

Surface reconstructions which we consistently produce include the $(1\times1)$, $(2\times4)$, $(4\times2)$-$c(8\times2)$, $(4\times6)$, and, at temperatures approaching the onset of surface decomposition, a pattern characteristic of surface facetting. Photoemission measurements, in conjunction with detailed line-shape analysis,[21] show subtle and systematic changes in the Ga 3*d* and As 3*d* core-level features with desorption temperature, in good agreement with previous studies.[20,22] Relative intensity of these core-level features indicates a large compositional change between the As-rich $(1\times1)$ surface annealed at 360 °C and the Ga-rich $(4\times2)$-$c(8\times2)$ reconstruction at the threshold of surface decomposition, analogous to that previously reported for as-grown MBE-GaAs(100) surfaces.[6] The surface Fermi level remains $\sim 0.6$ eV above the valence-band maximum ($E_v$) throughout the 500–600 °C temperature range of the $(4\times2)$-$c(8\times2)$ reconstruction. For very As-rich and for slightly decomposed surfaces, $E_F$ moves toward $E_v$. This movement, measured by the shifts of the Ga 3*d* and As 3*d* substrate core-level components, does not exceed $\sim 120$ meV. These changes in the $E_F$ position correlate well with cathodoluminescence spectroscopy (CLS) results which find corresponding variations in deep-level emission energy between different surface reconstructions.[23,24] In contrast, our photoemission measurements show large changes in the surface ionization potential and work function between different surface reconstructions, analogous to those previously reported on as-grown MBE-GaAs(100) surfaces.[25,26] We demonstrate that this large sensitivity of work function to local atomic ordering

 ©1992 The American Physical Society

provides an important indicator of surface homogeneity. Coupled with the variations in deep-level features, these work-function measurements emphasize the importance of surface processing on the electronic structure of the clean GaAs(100) surfaces.

## II. EXPERIMENT AND DATA ANALYSIS

Soft-x-ray photoemission (SXPS) experiments were performed at the Synchrotron Radiation Center of the University of Wisconsin using the 6-m toroidal grating monochromator (TGM) and beamline. Photoelectrons were collected by a double pass cylindrical mirror analyzer with overall energy resolution in the 0.25–0.45-eV range. Ga 3*d* and As 3*d* core-level spectra were excited with 80- and 100-eV photons, respectively, and the valence-band (VB) emission was monitored using 57-eV incident photon energy. Photoemission measurements of the surface ionization energy were carried out using 22-eV photons and by biasing the sample negatively ( $-7$ V) relative to the analyzer. Surface ionization energy was then derived from the energy separation between the top (highest kinetic energy) of the valence-band edge and the low-energy cutoff of the secondary electron emission, both determined by linear extrapolation of the spectral edge to the background line.[27,28]

Core-level photoemission spectra were analyzed on a minicomputer using a standard nonlinear least-squares line-shape fitting routine.[21] Both the As 3*d* and Ga 3*d* spectra were fit with a pair of symmetric spin-orbit doublets formed by convolution of the Lorentzian and Gaussian line shapes. These doublets were superimposed onto a secondary electron background approximated with a cubic polynomial and subsequently fit to the original spectra through a minimum of 300 iterations. Lorentzian widths (defined as full width at half maximum) and the spin-orbit splitting were fixed at 155 (180) meV and 445 (690) meV for each of the Ga 3*d* (As 3*d*) spectra, respectively.[22,29] The remaining parameters, i.e., the Gaussian width, kinetic energy, intensity, and branching ratio, were allowed to vary freely. Their values were obtained as an outcome of the fitting process. In analogy with the fitting procedure described in Refs. 22 and 29, we maintained equal branching ratios and Gaussian widths between the substrate and the surface-shifted components. However, we did not find it necessary to fix the energy separation between the As and Ga substrate components while fitting core-level spectra corresponding to different desorption temperatures.[29]

The *n*-type Si-doped ($N_d = 7\times 10^{16}$ cm$^{-3}$) GaAs(100) surfaces were prepared at the IBM-Yorktown Heights facility by MBE growth on top of chemically etched GaAs(100) substrates. Before removal from the MBE chamber, the surfaces were encapsulated with a relatively thick ( $>1000$-Å) layer of amorphous As and then shipped to the Xerox Webster Research Center under vacuum. Finally, clean surfaces, free of oxygen and carbon contamination, were produced by thermal desorption of As in vacuum chambers equipped with ion and cryogenic pumps maintaining pressure in the low-$10^{-10}$ Torr range. We carried out sequential As desorptions, gradually increasing the temperature at each step. Desorption cycles consisted of a nearly linear temperature ramp ( $\sim 5-10$ °C/s) with a $\sim$5-s anneal at the maximum temperature; the power was then turned off and the sample allowed to cool down to the ambient temperature. Each cycle was followed by SXPS and LEED measurements. To isolate the possible effects of the electron beam on these surfaces, separate runs were carried out without the use of LEED. No significant differences in the $E_F$ position were observed between such runs.

## III. RESULTS AND DISCUSSION

### A. Surface reconstruction and chemistry

Figure 1 shows representative LEED patterns obtained at *in vacuo* decapped GaAs(100) surfaces. The $(1\times1)$ pattern, shown in Fig. 1(a), is typically observed for desorption temperatures between $\sim$350 and 400 °C and corresponds to a very As-rich surface, likely terminated with a few monolayers of physisorbed As.[6] For temperatures between $\sim$400 and 480 °C, LEED reveals a $(2\times4)$-$c(2\times8)$ surface structure produced by dimerization of the terminating As layer, with each surface cell containing either one or two missing As dimers [Fig. 1(b)].[8–10] The sharpness of this pattern deteriorates close to the boundaries of the above temperature range. In addition, for desorption temperatures between 450 and 500 °C, we occasionally observed superposition of the $(2\times4)$ and $(4\times2)$ patterns indicative of a gradual transition from As-rich to more Ga-rich surface reconstructions. For the relatively broad range of temperatures between $\sim$500 and 600 °C we obtain the well-defined $(4\times2)$-$c(8\times2)$ LEED patterns shown in Figs. 1(c) and 1(d). Here, Ga dimers are arranged in analogy to the As dimers at the $(2\times4)$-$c(2\times8)$ reconstruction, but with a dimerization direction rotated by 90°.[10] Again, the appearance of this pattern degrades toward both the low and high end of its desorption-temperature range. Ultimately, for annealing temperatures exceeding $\sim$620 °C, the GaAs(100) surface starts to decompose and partially recrystallize, which is revealed in the characteristic LEED pattern shown in Fig. 1(f).

Figure 1 also demonstrates the effects of the vacuum condition on surface ordering observed at decapped GaAs(100). First, comparison of the image in Fig. 1(b) with those in Figs. 1(c) and 1(d) reveals that the Ga-rich reconstruction is more well ordered and produces a sharper LEED pattern than its As-rich counterpart. This difference is especially evident under optimal vacuum conditions, i.e., with the As background pressure below $\sim 4\times10^{-10}$ Torr. Second, Fig. 1(e) shows the $(4\times6)$ surface reconstruction which appears only when we allow the As background pressure to rise above $\sim 1\times10^{-9}$ Torr. This $(4\times6)$ pattern then replaces the expected $c(8\times2)$ reconstruction for temperatures above $\sim$580 °C and persists with annealing until the surface becomes fully decomposed. The $(4\times6)$ LEED pattern arises as a superposition of the contributions from the $(4\times1)$- and $(2\times6)$-reconstructed surface domains.[10] Our photoemission measurements indicate that the $(4\times6)$ surfaces are $\sim$10% more As rich than the $c(8\times2)$ surfaces produced at identical temperatures.

Another indicator of the effect of As background pres-

sure on surface reconstruction is the absence of the $c(4\times4)$ reconstruction in our UHV surface annealing sequence. Based on its atomic composition, this reconstruction is expected to appear for desorption temperatures separating the $(1\times1)$ and $(2\times4)$-$c(2\times8)$ temperature regions.[6,10] However, Biegelsen *et al.* deliberately exposed GaAs surfaces to $As_2$ or $As_4$ flux in order to produce the $c(4\times4)$ reconstruction, in sharp contrast to our procedure which allows only a small presence of As in vacuum.[10] The absence of the $c(4\times4)$ surface reconstruction in UHV conditions, as well as the appearance of the $(4\times6)$ reconstruction under increased As partial pressure, clearly point to the importance of As background pressure for preparation of thermally decapped GaAs(100) surfaces.

In Fig. 2 we show changes in local bonding at decapped GaAs(100) surfaces as a function of As desorption temperature and surface reconstruction. Representative

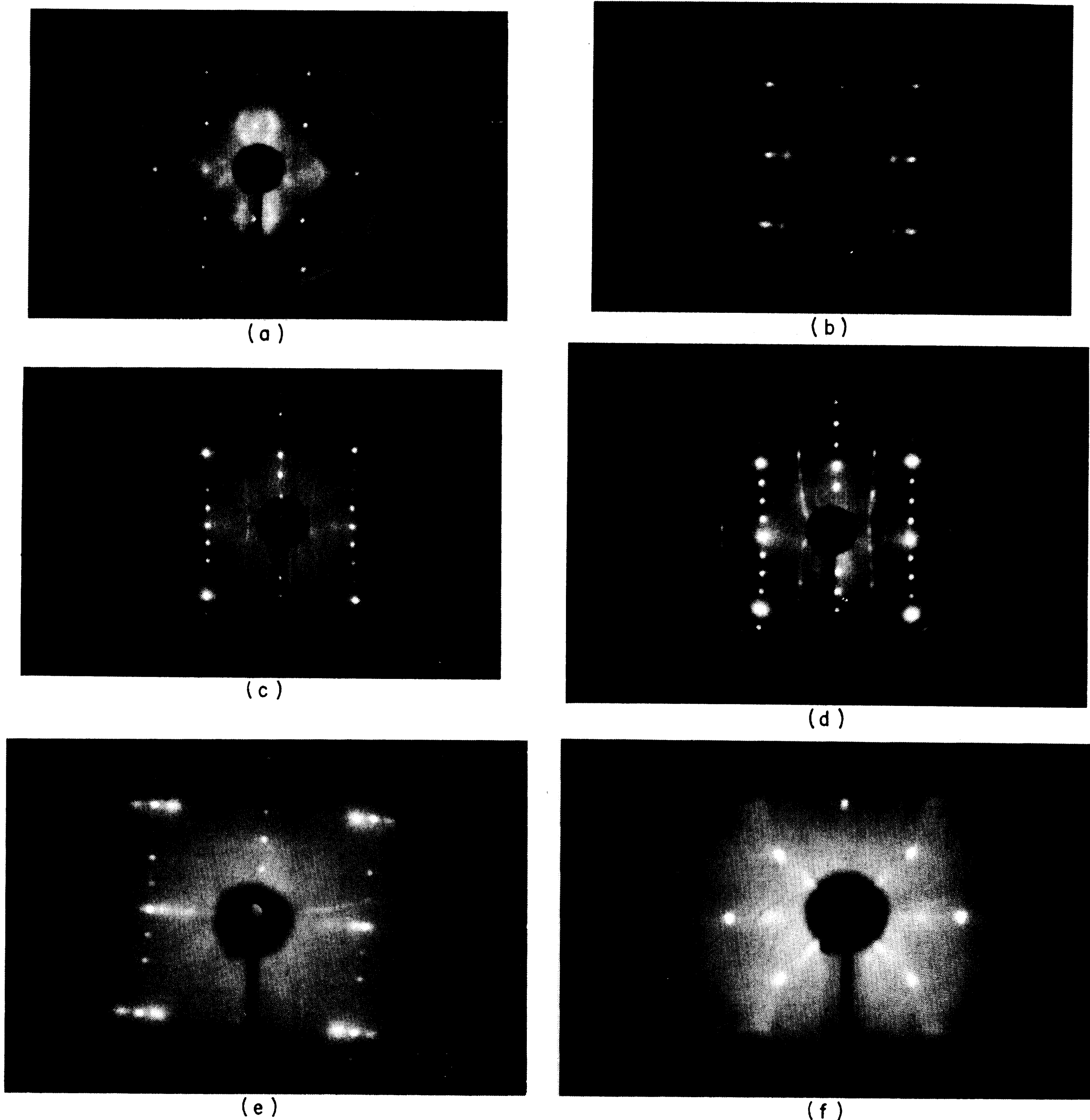

FIG. 1. Characteristic LEED spectra from decapped GaAs(100) surfaces: (a) $(1\times1)$ at 350 °C; (b) $(2\times4)$-$c(2\times8)$ at 420 °C; (c) $(4\times2)$-$c(8\times2)$ at 520 °C; (d) $(4\times2)$-$c(8\times2)$ at 580 °C; (e) $(4\times6)$ at 600 °C; (f) the "star burst" pattern revealing surface decomposition.

Ga 3*d* spectra in Fig. 2(a) were taken at 80-eV incident photon energy, with an estimated escape depth of ~5 Å.[30] Line-shape decomposition of these spectra shows the presence of a substrate Ga 3*d* component (sub) and of two surface-shifted components, ss1 and ss2, at the high and low binding-energy side of the substrate, respectively. As described in Sec. II, Gaussian widths of the three components were maintained equal for each surface, but allowed to vary between surfaces prepared at different temperatures.[18,22] The Gaussian width varied between 480 and 580 meV in a somewhat oscillatory manner as the desorption temperature was gradually increased. Such variations also occurred within a temperature range corresponding to a single surface reconstruction and correlated well with the changing sharpness of a particular LEED pattern. The narrowest line shape was found to correspond to the sharpest and best defined LEED image. Binding energies relative to the substrate feature and intensities of the surface-shifted components also showed systematic variations with the annealing temperature: the relative binding energy of the ss1 component decreased from 0.62±0.02 eV for the 360 °C annealed (1×1) surface to 0.54±0.02 eV for the (4×2)-*c*(8×2) surfaces obtained in the 500–580 °C temperature range. Simultaneously, the relative binding energy of the ss2 component changed from −0.45±0.02 eV to −0.40±0.02 eV between these surface reconstructions.

Perhaps the most striking feature in the Ga 3*d* line-shape evolution with desorption temperature is the nearly complete absence of the ss2 contribution from the As-rich (2×4) surfaces annealed to below ~480 °C. For these surfaces, the ss1 component is relatively prominent, contributing ~24% of the total integrated intensity. For temperatures between ~500 and 600 °C and the more Ga-rich (4×2)-*c*(8×2) reconstruction, each of the surface-shifted components contributes ~10% of the total Ga 3*d* emission. At temperatures above ~620 °C, as the GaAs(100) surface begins to decompose, dissociated As sublimes from the surface and dissociated Ga atoms start to aggregate into clusters at the surface.[18,22] Indeed, the top spectrum in Fig. 2(a) indicates the formation of a new component which is displaced −0.71±0.02 eV relative to the substrate. The Gaussian width of this component is just 280 meV, as compared to 510-meV Gaussian width of the substrate component. This new component is also observed to grow in relative intensity, shar-

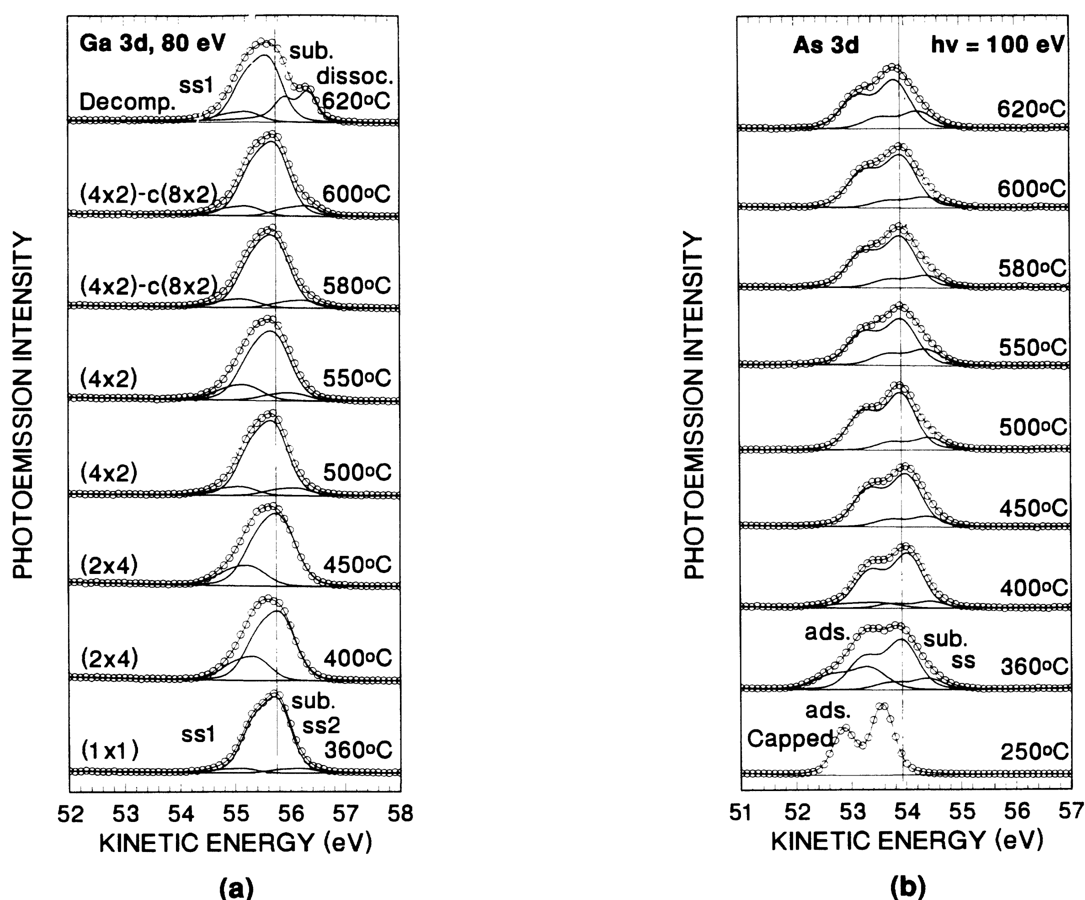


FIG. 2. Effect of desorption temperature and reconstruction on (a) Ga 3*d* and (b) As 3*d* surface-sensitive photoemission spectra for clean GaAs(100). Ga 3*d* core levels show two surface-shifted components, ss1 and ss2, as opposed to a single surface component of the As 3*d* spectra. Incipient surface decomposition produces a distinct component at the low binding-energy side of Ga 3*d* emission.

pen, and shift to lower binding energy as the surface is further annealed to higher temperatures. It exhibits the Doniach-Sunjic line-shape asymmetry characteristic of a metallic environment, with the asymmetry parameter $\alpha=0.09\pm0.01$.[31] These characteristics indicate that this core-level feature can be associated with the Ga droplets that begin to form at thermally decomposed surfaces.[18,22]

Figure 2(b) illustrates the changes in the surface-sensitive As $3d$ core-level energy distribution curves (EDC's) with desorption temperature. The 250 °C desorption removes the top oxidized portion of the As film, with enough residual As to screen out the substrate photoemission signal. This clean As film results in a well-resolved single-component As $3d$ core-level spectrum. Further surface annealing to 360 °C results in a core-level emission composed of three spin-orbit doublets: a substrate (sub) component, a surface-shifted (ss) component displaced by $0.47\pm0.02$ eV to lower binding energy, and a third component (ads) at the high binding-energy side of the spectrum. This third component is relatively broad and, by comparison with the 250 °C spectrum in Fig. 2(b), it can be attributed to the residual As on the surface. The large Gaussian width of this component arises from inequivalent bonding sites of absorbed as atoms, as compared to the homogeneous local environment in bulk As film evidenced in the 250 °C spectrum. Significantly, both the 0.60-eV relative shift and the relative intensity of the absorbed As contribution in the 360 °C spectrum correspond closely to the results of van der Ween *et al.*[32,33] and Ludeke, Chiang, and Eastman[34] obtained at the $c(4\times4)$ surfaces prepared and studied *in situ* in a MBE-growth chamber. The discrepancy between our $(1\times1)$ LEED pattern and the $c(4\times4)$ pattern observed by those investigators at surfaces with nearly identical chemical composition is not well understood and likely reflects the subtle differences between their as-grown and our decapped GaAs(100) surfaces.[35] The adsorbed component typically vanishes at surfaces annealed above 400 °C. Its presence, however, is found to depend sensitively on both the As background pressure and the duration of annealing. Thus, when the As partial pressure was increased to above $1\times10^{-9}$ Torr, a sequence of several rapid anneals produced a surface with adsorbed As even for the 550 °C final desorption temperature.

Line-shape analysis in Fig. 2(b) also shows that the surface-shifted component becomes more pronounced and changes its relative position with increasing desorption temperature. Average relative binding energies of this component are $0.40\pm0.02$ eV for the $(2\times4)$ reconstruction, and $0.47\pm0.02$ eV for the $(4\times2)$ surface reconstruction, respectively. Corresponding contributions of the surface-shifted components to the total As $3d$ emission intensity increase from $\sim13\%$ for the $(2\times4)$ to $\sim22\%$ for the $(4\times2)$-$c(8\times2)$ reconstruction. These changes reflect a gradual change in local bonding of surface As atoms between the As-dimer and Ga-dimer-terminated surface reconstructions.[29]

In spite of the rather detailed knowledge of surface atomic arrangements at reconstructed GaAs(100) surfaces afforded by LEED and scanning tunneling microscopy (STM) studies,[8,10] definitive assignment of surface-shifted components of the Ga $3d$ and As $3d$ core-level emissions is not possible before the electronic structure calculations for these reconstructed surfaces become available. For the Ga-dimer-terminated $(4\times2)$-$c(8\times2)$ surface, Le Lay *et al.* proposed that the two surface-shifted Ga $3d$ features ss1 and ss2 correspond to surface Ga atoms in dimers localized between the two neighboring Ga dimers, and next to a missing Ga dimer, respectively.[29] However, this tentative assignment was made under the assumption of a single missing dimer per $(4\times2)$ unit cell, in contrast to the recent STM study of Biegelsen *et al.*, who observed $(4\times2)$ unit cells consisting of two Ga dimers adjacent to one another and two missing dimers.[10] Furthermore, the prominence of the Ga $3d$ ss1 surface-shifted component for the As-rich $(2\times4)$ surfaces in Fig. 2(a) demonstrates that this feature is not unique to dimerized Ga atoms at the surface. Indeed, a similar surface-shifted component (although with a smaller energy shift relative to the substrate) is commonly observed for the cleaved GaAs(110) surfaces.[30] The latter surfaces also exhibit a single As $3d$ surface-shifted feature analogous to the ss component in Fig. 2(b) spectra.[30] Overall, we conclude that the surface-shifted components at GaAs(100) surfaces reflect the existence of inequivalent, reconstruction-dependent bonding sites of surface and subsurface atoms. Whereas relative intensities, binding energies, and Gaussian widths of these spectral features provide a useful tool for identifying structural and electronic characteristics of these surfaces, the precise assignment of surface-shifted components to specific bonding sites at these surfaces falls beyond the means of our current theoretical and experimental capabilities.

We can gain further insight into the changes in GaAs(100) surface composition by monitoring total photoemission signal intensities from Ga and As atomic species. Figure 3 shows plots of the As $3d$ and Ga $3d$ emission intensity ratios as a function of desorption temperature and surface reconstruction obtained in two desorption experiments. Emission intensities are obtained as a total background-subtracted area of the line-

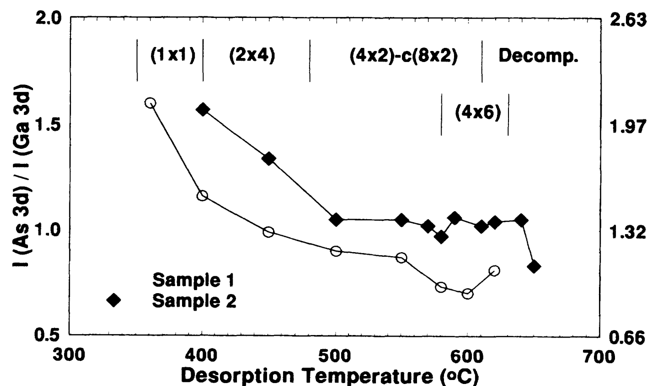


FIG. 3. Total emission intensity ratio between the As $3d$ and Ga $3d$ core-level spectra as a function of desorption temperature and surface reconstruction (designated at the top of the figure). The scale on the right-hand side reflects the adjustment for the core levels' ionization cross-section difference, explained in the text.

shape-analyzed spectra. The right-hand scale shows the As 3*d*/Ga 3*d* ratio with the core-level emission intensities normalized to their respective ionization cross sections.[36] Such normalization reflects surface composition more realistically and provides a possibility to compare data collected at different photon energies. Both sets of data in Fig. 3 show gradual reduction of the As-to-Ga atomic ratio with annealing temperature for temperatures below ~500 °C, and a relative saturation of this ratio for higher temperatures. The As 3*d*/Ga 3*d* ratio ranges from ~1.6 for the (1×1) reconstruction to between 0.8 and 1.0 for the (4×2)-*c*(8×2) reconstruction, in good agreement with previous measurements.[6] It is important to note that even within the well-defined *c*(8×2) reconstruction, significant variations in surface stoichiometry may occur as a function of surface processing. Such variations are reflected in the difference of the average atomic ratio for the *c*(8×2) surface observed between the two sets of data in Fig. 3, as well as in the changes of the As/Ga ratio between successive anneals. Significantly, each of the plots shows a local minimum in the As 3*d*/Ga 3*d* ratio within the (4×2)-*c*(8×2) temperature range which corresponds to the most Ga-rich *c*(8×2) surface. Annealing beyond this temperature increases again the As content of the surface, either through readsorption of As or by its outdiffusion from the substrate. We believe that As readsorption plays a somewhat more important role since deliberate exposure to increased As background pressure ($1\times10^{-9}$ Torr) did not only increase the As-to-Ga ratio, but it also produced a different, (4×6) surface LEED pattern. The temperature range of this (4×6) pattern is shown in the top of Fig. 3. Annealing beyond ~630 °C leads to further depletion of As from the GaAs(100) surfaces.

### B. Valence-band spectra and surface $E_f$ position

Figure 4 shows GaAs(100) valence-band (VB) spectra collected at 47-eV photon energy from surfaces annealed in the 360–620 °C temperature range. The vertical dashed line, positioned at 41.28-eV kinetic energy, corresponds to the average valence-band maximum ($E_v$) of the 500, 550, and 580 °C spectra. The equilibrium $E_F$ position for our analyzer, obtained with a Au reference, was at 41.90±0.05 eV for the 47-eV photon energy.

Valence-band spectra show significant changes with desorption temperature and surface reconstruction. In particular, the high-kinetic-energy end of VB spectra (the VB edge) is very sensitive to surface reconstruction. Thus, the 400 °C spectrum in Fig. 4 shows an especially sharp edge, possibly due to the presence of a surface state. This dangling-bond-derived surface state has been previously observed on As-rich *c*(4×4) surfaces.[32] As expected, this state vanishes for higher desorption temperatures causing the VB edge to maintain a uniform appearance in the 450–580 °C temperature range. For desorptions above 600 °C, the VB edge becomes less well defined as additional emission starts to appear at energies above the established VB maximum (dashed line in Fig. 4). Based on the simultaneous changes which occur in the Ga 3*d* core-level spectra in this temperature range, we associate the new emission with metallic states produced by Ga clusters on the surface.

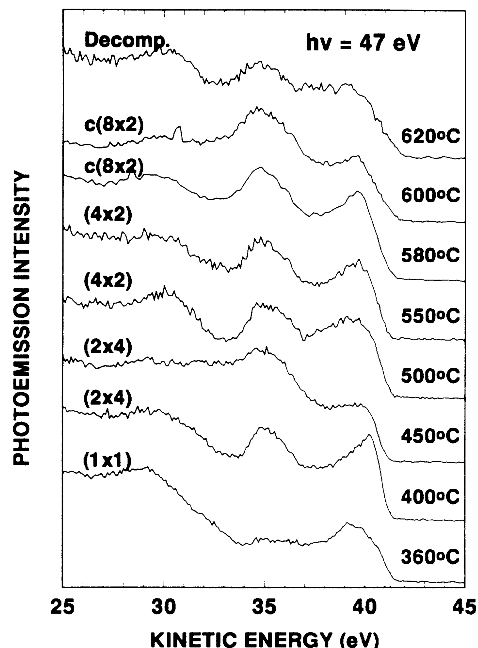


FIG. 4. Valence-band spectra show relatively minor changes between different surface reconstructions. The most pronounced changes occur near the top of the valence-band emission, which is especially short for the 450 °C spectrum.

Valence-band-edge modification by the presence of either surface states at As-rich surfaces or metallic states at slightly decomposed surfaces introduces some uncertainty into $E_F$ position measurements at GaAs(100) clean surfaces and interfaces.[27] Figure 5 illustrates this by showing two sets of results extracted from photoemission spectra presented in Figs. 2 and 4. Filled squares represent $E_F$ positions determined by measuring directly the energy difference between the point at which the extrapolated leading VB edge intersects the spectral baseline and the equilibrium Fermi-level position

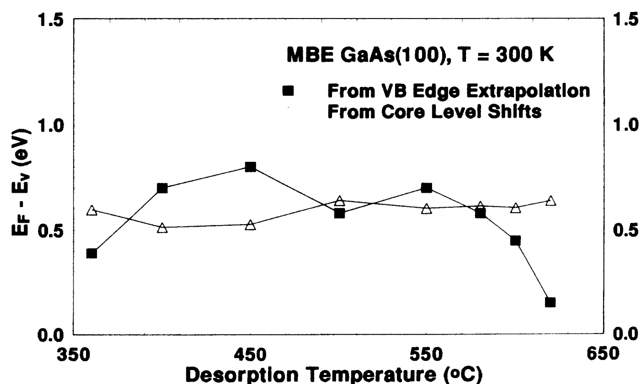


FIG. 5. Desorption-temperature dependence of the surface Fermi-level position measured by (a) direct valence-band-edge extrapolation (solid squares), and (b) changes in Ga and As core-level energies. The latter minimizes effects of the changes in the VB-edge emission with desorption temperature and indicates relatively little $E_F$ movement between differently reconstructed surfaces.

(41.90±0.05 eV). The $E_F$ position established in this way moves from 0.4 eV above the $E_v$ for the 360 °C desorption to the maximum ($E_F$-$E_v$) value of ~0.8 eV for the 450 °C desorption, and then varies between 0.6 and 0.7 eV for desorption temperatures between 500 and 580 °C. At even higher temperatures, as the surface becomes progressively decomposed, the $E_F$ appears to rapidly approach $E_v$. This apparently erratic Fermi-level movement with desorption temperature is predominantly an artifact of the surface-chemistry-induced changes in VB-edge emission discussed in the previous paragraph. As we point out next, it is not in good agreement with the $E_F$ movement measured from rigid shifts of the Ga and As core levels.

The second plot (open triangles) in Fig. 5 shows $E_F$ movement based on a consistent use of both the VB-edge spectra and the Ga 3*d* and As 3*d* core levels. We started by selecting a set of "optimal" VB's corresponding to surfaces desorbed at 500, 550, and 580 °C, and from those established an average reference ($E_F$-$E_v$) offset of 0.62 eV. We then extracted changes in band bending relative to these surfaces by measuring rigid shifts of the substrate component of the analyzed As 3*d* and Ga 3*d* core-level spectra. This method produced a relatively stable ($E_F$-$E_v$) measurement of 0.62±0.05 eV for surfaces annealed between 500 and 620 °C, and 0.52±0.05 eV for the As-rich (2×4) surfaces produced by the 400 and 450 °C desorptions. The $E_F$ stabilization energy observed for the $c(8\times2)$ surface agrees very well with similar measurements performed by other groups.[22] It should also be pointed out that, for desorption temperatures in excess of ~620 °C, we commonly observe further $E_F$ movement toward the valence-band maximum. This movement is likely caused by the formation of thermally generated defects in GaAs located ~0.5 eV above $E_v$.[23]

The discrepancy between the core-level-analysis-based ($E_F$-$E_v$) measurements and similar measurements performed exclusively by VB-edge extrapolation is, as shown in Fig. 5, more emphasized for lower-temperature-annealed surfaces. Indeed, our VB-edge extrapolation for the (2×4) As-rich surfaces prepared in the 400–500 °C temperature range suggests a relative $E_F$ position of 0.7–0.8 eV above $E_v$, in good agreement with the previous results of Svensson *et al.*[37] and Chen *et al.*[38] Our core-level analysis, however, yields ($E_F$-$E_v$) values of ~0.52 eV, which suggests that As-terminated surfaces are more, rather than less "pinned" than their Ga counterparts. Both core-level spectra, analyzed with an appropriate line-shape fitting routine, and VB-edge extrapolation are commonly used in determining at least one reference value for the ($E_F$-$E_v$) separation in photoemission experiments. Thus these different procedures may contribute, along with the different surface processing and GaAs growth conditions, to the variation in clean surface $E_F$ positions reported in different photoemission studies of reconstructed GaAs(100) surfaces.

### C. Surface-work function

We have measured the decapped GaAs(100) surface-work function for different surface reconstructions and desorption temperatures. These measurements consisted of first determining the surface ionization energy (not shown) from the energy difference between the valence-band maximum and the low-energy cutoff of the secondary photoelectron emission.[27,28] The work function is then obtained by subtracting ($E_F-E_v$) from the ionization energy for each desorption temperature:

$$\Phi=I-(E_F-E_v)=h\nu-\Delta-(E_F-E_v)\ , \quad (1)$$

where $\Phi$ denotes the surface work function, $I$ the ionization energy, $h\nu$ the incident photon energy, and $\Delta$ the energy separation between the valence-band maximum and the low-energy cutoff of secondary photoelectrons.

In addition to the uncertainty in determination of the VB edge discussed in the previous section, surface-work-function measurements were complicated by the presence of multiple structures near the cutoff of the secondary electron emission, shown in Fig. 6. Solid arrows in Fig. 6 indicate the lowest kinetic-energy cutoff (corresponding to a low work-function value), while the open arrows mark the second, higher kinetic-energy photoemission cutoff (corresponding to a higher surface-work function). The presence of two cutoffs likely reflects coexistence of surface phases (patches) with distinctly different ionization energies.[27] Indeed, the previously discussed variations in the surface core-level widths and LEED pattern sharpness suggest that transitions between different surface reconstructions occur gradually with desorption temperature.[35] The relatively constant ~0.8-eV separation between the two cutoffs suggests that each of them corresponds to a well-defined and stable surface configuration, possibly one with the As dimer and the other with the Ga dimer termination.[5,35,38] It is noteworthy that both the

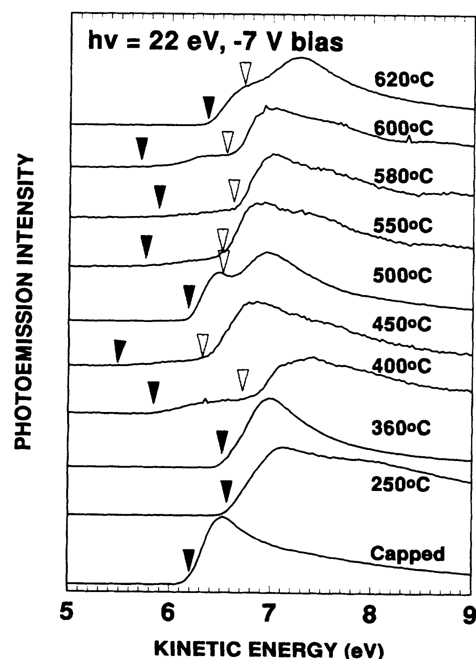


FIG. 6. Secondary electron emission cutoffs obtained with 22-eV photon energy and −7-V sample bias relative to the ground. The two cutoffs indicated by the solid and empty arrows reflect the presence of surface inhomogeneities.

relative emission intensities and energies corresponding to these two cutoffs change with desorption temperature. The relative prominence of the cutoffs may reflect the relative concentration of their corresponding surface domains and is expected to vary sensitively with temperature, heating cycle duration, and As background pressure during desorptions. The variations of the single or multiple EDC cutoffs reflects the appearance of phases with new reconstructions and chemical composition. Depending on their spatial extent, such phases may interact through their space-charge regions, averaging the surface electronic properties on a microscopic scale. Based on the variable sharpness of the otherwise similar LEED patterns within a particular reconstruction range of temperatures, we speculate that such patches are of dimension comparable to or smaller than the coherence length of the diffracted LEED beams, (e.g., several hundred Å). In general, the absolute values of ionization energy and work function appear to be a function of the surface reconstruction and chemical composition, as well as microscopic structural and chemical inhomogeneity.

Figure 7 presents work-function data based on the position of the first cutoff (solid triangles, dashed line), the second cutoff (open circles, dashed line), and their weighted average (solid diamonds, solid line). The latter was calculated by weighting each of the work-function values with the normalized peak emission intensity of the corresponding energy cutoff. Under the assumption that the maximum emission intensity preceding each cutoff scales linearly with the surface area covered by its associated surface phase, this is equivalent to weighting each of the work-function values with the percentile of surface covered with its corresponding domains.[27,39] This normalization procedure should, to some extent, facilitate comparison of our data with those obtained by the contact potential difference,[25,28] photoionization threshold,[26] or a space diode technique.[36] For desorption temperatures up to 400 °C, only a single cutoff is observed in the secondary electron spectra (Fig. 6), indicative of surface termination by at least a monolayer of adsorbed As.

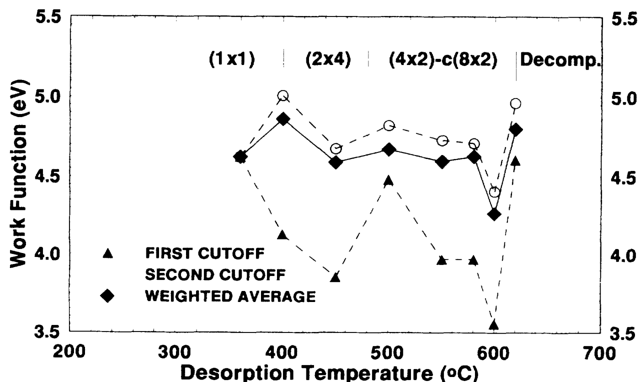


FIG. 7. GaAs(100) surface-work function changes with desorption temperature and surface reconstruction. Dashed plots correspond to work-function values determined from the positions of either of the two cutoffs shown in Fig. 6. The solid plot corresponds to the surface-averaged work function.

Significantly, there is a large shift in the cutoff energy between the starting air-exposed capped surface and the same surface annealed to 250 °C and therefore covered with a thick layer of clean As. However, the latter exhibits a nearly identical cutoff energy as the $(1\times1)$ surface with only a few monolayers of As coverage. The surface annealed to 400 °C presents a weak $(2\times4)$ pattern and two cutoffs indicative of surface inhomogeneity, which is likely due to residual surface As.[36] Between 400 and 450 °C, both cutoffs shift to lower kinetic energy revealing a decrease in the surface-work function, which reaches a local minimum at 450 °C. This is in general agreement with the previously reported trends of work-function change with As coverage, although this local minimum is commonly associated with the $c(4\times4)$ reconstruction which we are unable to produce at decapped surfaces.[25,26,36,38]

After a 500 °C desorption, the first cutoff in Fig. 6 shifts by ~0.5 eV which, taking into account the simultaneous change in band bending, yields a 0.63-eV increase in the associated surface-work function. This large work-function change resembles the abrupt transition between the $c(4\times4)$ and $c(2\times8)$ surface-work functions first reported by Massies, Devoldere, and Linh.[25] However, the 500 °C spectrum in Fig. 6 exhibits a very pronounced double cutoff structure possibly reflecting the simultaneous presence of both the As-rich $c(2\times8)$ and the Ga-rich $(4\times2)$ patches at the surface. Indeed, the weighted average work function in Fig. 7 shows only ~80-meV change between the 450 and 500 °C data points, which suggests that the 500 °C anneal in our experiment produced a surface outside the narrow temperature range corresponding to the "pure" $c(2\times8)$ reconstruction, so that the associated maximum in the surface-work function was not pronounced.[35] Work-function behavior for desorption temperatures between 500 and 600 °C is in excellent agreement with the previous[25] and recent[35,38] work in that it shows a gradual decrease, a plateau, and then a further decrease to the absolute minimum which occurs at the high-temperature limit of the $c(8\times2)$ reconstruction. Surface annealing beyond 600 °C causes the work function to rise again as the surface continues to lose As and gradually decompose. Surface decomposition is accompanied with the formation of dissociated Ga clusters which introduce new structure into the secondary electron emission spectra (Fig. 6, top spectrum).

Overall, these results demonstrate high sensitivity of the GaAs(100) work function to surface reconstruction as well as desorption temperature within a given reconstruction. Significant changes in the surface work function arise nearly completely from changes in the ionization energy since the Fermi-level movement does not exceed ~120 meV in this temperature range. The ionization energy is most likely determined by the orientation, as well as the relative concentration of the surface dipoles caused by the polar character of GaAs(100) surfaces.[26,27] Chen *et al.* used a simple electron-counting model to propose that the direction of the dipole is perpendicular to the surface and that its orientation changes by 180° between the As-dimer-terminated $(2\times4)$-$c(2\times8)$ and Ga-dimer-

terminated $(4\times2)$-$c(8\times2)$ surfaces.[38] Our results indeed show a large (0.4 eV for the average, and 0.9 eV for the work function based on the first cutoff) work-function variation between these surfaces. However, our results also demonstrate that the actual surfaces are far from the ideal ones in that they simultaneously contain patches with distinctly different values of the ionization energy and work function. Our most recent studies indicate that surface inhomogeneity, reflected in the presence of multiple secondary electron cutoffs, persists even after prolonged ($\sim$15-min) surface anneals at a given temperature, although the relative intensity of the near-cutoff emission features varies with the annealing time. Thus, the relative concentration of the reconstructed (or As-covered) surface patches changes with desorption temperature, the duration of the annealing, and with the associated surface composition, providing for the observed gradual changes in the surface work function.[25,35,38]

## IV. CONCLUSIONS

Chemical, structural, and electronic properties of decapped GaAs(100) surfaces vary systematically with surface desorption temperature. Surface reconstruction depends on processing conditions, most sensitively on the desorption temperature, As background pressure, and duration of annealing cycles. Core-level and valence-band photoemission spectra show subtle but important changes with desorption temperature and surface reconstruction. Valence-band-edge emission is particularly sensitive to these parameters and should therefore be used cautiously in relative Fermi-level position measurements. Surface $E_F$ lies $0.62\pm0.05$ eV above $E_v$ for the more Ga-rich surfaces annealed to between 500 and 620 °C, and $0.52\pm0.05$ eV for the As-rich $(2\times4)$ surfaces produced by the 400 and 450 °C desorptions. The $E_F$ position at various desorption temperatures appears related to changes in surface deep levels measured by cathodoluminescence spectroscopy (not shown). Atomic composition, determined by the As 3*d* to Ga 3*d* total intensity ratio, varies predictably with desorption temperature. The wide ranges of chemical composition, as well as the variable sharpness of core levels and surface LEED patterns within a single reconstruction suggest the appearance of multiple phases at the GaAs(100) surface. Such surface inhomogeneities are evidenced by multiple features in the near-cutoff structure of secondary-emission spectra, which can also account for differences in the absolute magnitude of work-function variations between different techniques. Finally, it is worth noting that low-energy cathodoluminescence spectroscopy results presented elsewhere[40] reveal the presence of multiple deep levels, whose energies and densities also depend upon reconstruction and/or composition. Overall, a complement of UHV techniques reveal the sensitive dependence of the structural, chemical, and electronic properties of GaAs(100) on the specifics of surface processing and therefore provide us with a benchmark needed for reproducible preparation of these surfaces.

## ACKNOWLEDGMENTS

The authors wish to acknowledge the assistance of D. F. Rioux and the SRC Staff in photoemission measurements performed at the Synchrotron Radiation Center of the University of Wisconsin–Madison, which is a NSF-supported facility. We are also indebted to Professor A. Kahn, Dr. C. J. Palmstrøm, and Professor J. H. Weaver for providing their results prior to publication. This work was in part supported by the Office of Naval Research Contract No. N00014-91-C-0037.

[1] A. Y. Cho, J. Appl. Phys. **42**, 2074 (1971).
[2] A. Y. Cho, J. Appl. Phys. **47**, 2841 (1976).
[3] R. Ludeke and A. Koma, J. Vac. Sci. Technol. **13**, 241 (1976).
[4] P. Drathen, W. Ranke, and K. Jacobi, Surf. Sci. **77**, L162 (1978).
[5] J. Massies, P. Devoldére, and N. T. Linh, J. Vac. Sci. Technol. **15**, 1353 (1979).
[6] R. Z. Bachrach, R. S. Bauer, P. Chiaradia, and G. V. Hansson, J. Vac. Sci. Technol. **19**, 335 (1981).
[7] W. Mönch, in *Molecular Beam Epitaxy and Heterostructures, NATO Advanced Study Institute Series B: Physics* (Martinuus Nijhoff, Dordrecht, 1985), Vol. 87, p. 331, and references therein.
[8] M. D. Pashley, K. W. Haberern, W. Friday, J. M. Woodall, and P. D. Kirchner, Phys. Rev. Lett. **60**, 2176 (1988).
[9] M. D. Pashley, Phys. Rev. B **40**, 10481 (1989).
[10] D. K. Biegelsen, R. D. Bringans, J. E. Northrup, and L.-E. Swartz, Phys. Rev. B **41**, 5701 (1990).
[11] A. Appelbaum, G. A. Baraff, and D. R. Hamann, Phys. Rev. B **14**, 1623 (1976).
[12] D. J. Chadi, J. Vac. Sci. Technol. A **5**, 834 (1987).
[13] A. Y. Cho and P. D. Dernier, J. Appl. Phys. **49**, 3328 (1978).
[14] R. Ludeke, T.-C. Chiang, and D. E. Eastman, J. Vac. Sci. Technol. **21**, 599 (1982).
[15] L. J. Brillson, R. E. Vitturo, C. Mailhiot, J. L. Shaw, N. Tache, J. McKinley, G. Margaritondo, J. M. Woodall, P. D. Kirchner, G. D. Pettit, and S. L. Wright, J. Vac. Sci. Technol. B **6**, 1263 (1988).
[16] R. E. Viturro, J. L. Shaw, C. Mailhiot, L. J. Brillson, N. Tache, J. McKinely, G. Margaritondo, J. M. Woodall, P. D. Kirchner, G. D. Pettit, and S. L. Wright, Appl. Phys. Lett. **52**, 2052 (1988).
[17] R. E. Viturro, S. Chang, J. L. Shaw, C. Mailhiot, L. J. Brillson, A. Terassi, Y. Hwu, G. Margaritondo, P. D. Kirchner, and J. M. Woodall, J. Vac. Sci. Technol. B **7**, 1007 (1989).
[18] C. J. Spindt, M. Yamada, P. L. Meissner, K. E. Miyano, A. Herrera, A. J. Arko, and W. E. Spicer, J. Vac. Sci. Technol. B **9**, 2091 (1991).
[19] S. P. Wilks, J. I. Morris, D. A. Woolf, and R.H. Williams, J. Vac. Sci. Technol. B **9**, 2118 (1991).
[20] D. Mao, M. Santos, M. Shayegan, A. Kahn, G. Le Lay, Y. Hwu, G. Margaritondo, L. T. Florez, and J. P. Harbison, Phys. Rev. B **45**, 1273 (1992).
[21] J. J. Joyce, M. Del Guidice, and J. H. Weaver, J. Electron Spectrosc. Relat. Phenom. **49**, 31 (1989).
[22] G. Le Lay, D. Mao, A. Khan, Y. Hwu, and G. Margaritondo, Phys. Rev. B **43**, 14 301 (1991).

[23]I. M. Vitomirov, A. D. Raisanen, A. C. Finnefrock, R. E. Viturro, S. Chang, L. J. Brillson, P. D. Kirchner, G. D. Pettit, and J. M. Woodall, J. Vac. Sci. Technol. A **10**, 749 (1992).

[24]R. E. Viturro, J. L. Shaw, L. J. Brillson, J. M. Woodall, P. D. Kirchner, G. D. Pettit, and S. L. Wright, J. Vac. Sci. Technol. B **6**, 1397 (1988).

[25]J. Massies, P. Devoldere, and N. T. Linh, J. Vac. Sci. Technol. **16**, 1244 (1979).

[26]K. Hirose, E. Foxman, T. Noguchi, and M. Uda, Phys. Rev. B **41**, 6076 (1990), and references therein.

[27]W. Ranke, Phys. Rev. B **27**, 7807 (1983).

[28]D. W. Niles, M. Tang, H. Höchst, and G. Margaritondo, J. Vac. Sci. Technol. A **5**, 2057 (1987).

[29]G. Le Lay, D. Mao, A. Khan, Y. Hwu, and G. Margaritondo, Phys. Rev. B **43**, 14 301 (1991).

[30]M. C. Schabel, I. M. Vitomirov, G. D. Waddill, and J. H. Weaver, J. Electron Spectrosc. Relat. Phenom. **56**, 211 (1991).

[31]S. Doniach and M. Sunjic, J. Phys. C **3**, 285 (1970).

[32]J. F. van der Veen, P. K. Larsen, J. H. Neave, and B. A. Joyce, Solid State Commun. **49**, 659 (1984).

[33]J. F. van der Veen, L. Smit, P. K. Larsen, and J. H. Neave, Physica **117B & 118B**, 822 (1983).

[34]R. Ludeke, T.-C. Chiang, and D. E. Eastman, Physica **117B & 118B**, 819 (1983).

[35]R. Duszak, C. J. Palmstrøm, C. J. Sandroff, Y.-N. Yang, and J. H. Weaver, J. Vac. Sci. Technol. B **10**, 1891 (1992) and (private communication).

[36]J. J. Yeh and I. Lindau. At. Data Nucl. Data Tables **32**, 1 (1985).

[37]S. P. Svensson, J. Kanski, T. G. Andersson, and P.-O. Nilsson, J. Vac. Sci. Technol. B **2**, 235 (1984).

[38]W. Chen, M. Dumas, D. Mao, and A. Kahn, J. Vac. Sci. Technol. B **10**, 1886 (1992).

[39]This assumption is not generally exact in that measurement artifacts such as electric fields or the position of the sample surface relative to the acceptance cone of the cylindrical mirror energy analyzer may change the relative contributions from surface patches with different work functions. Furthermore, even in the absence of these artifacts the measurement is complicated by the presence of an absolute, surface-average vacuum level (and surface-work function) formed some distance above a heterogeneous surface. The existence of this physical surface-work function averaging impedes the determination of the high work-function component at heterogeneous surfaces.

[40]I. M. Vitomirov, A. D. Raisanen, A. C. Finnefrock, R. E. Viturro, L. J. Brillson, P. D. Kirchner, G. D. Petit, and J. M. Woodall, J. Vac. Sci. Technol. B **10**, 1898 (1992).

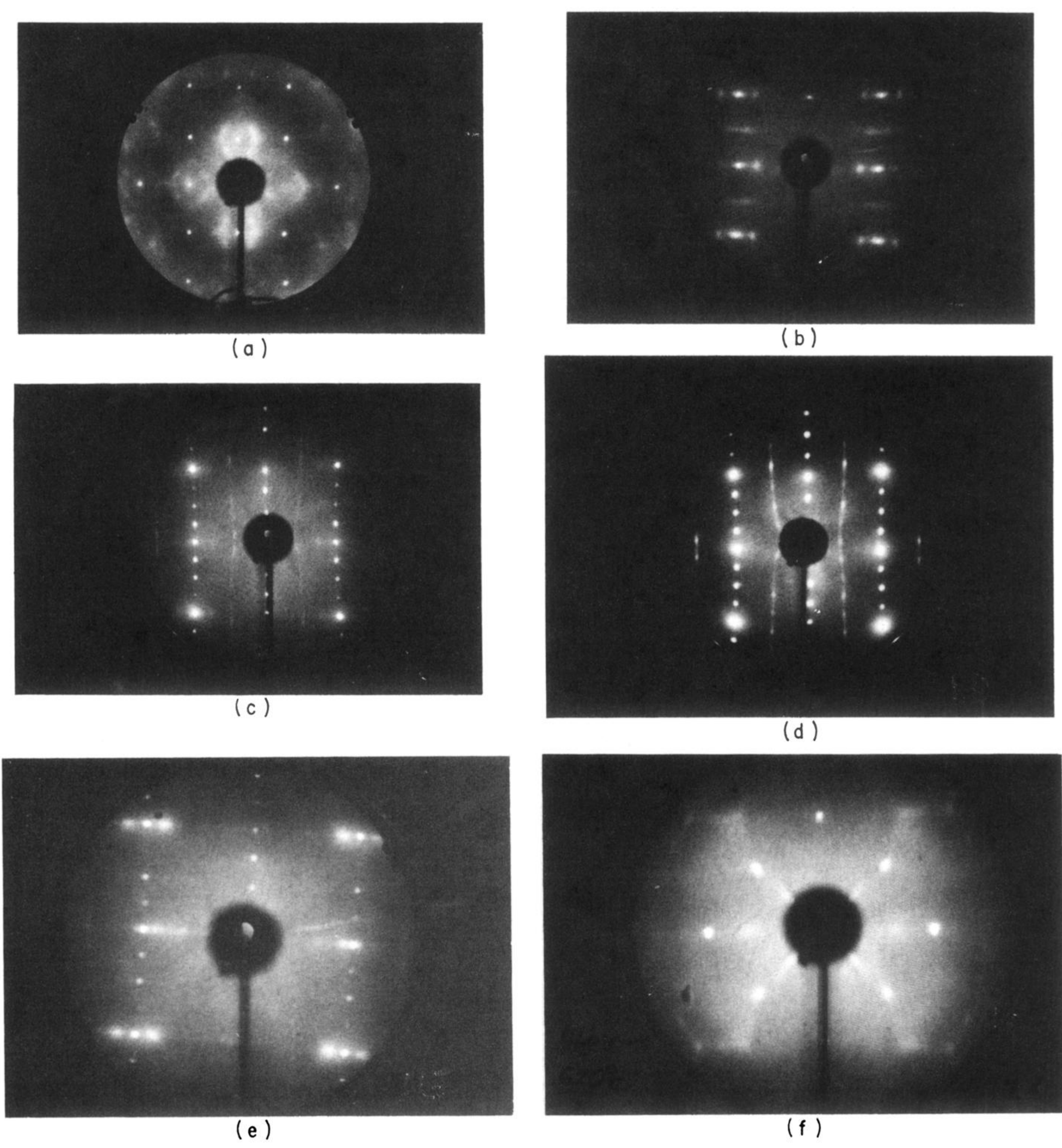


FIG. 1. Characteristic LEED spectra from decapped GaAs(100) surfaces: (a) (1×1) at 350 °C; (b) (2×4)-$c$(2×8) at 420 °C; (c) (4×2)-$c$(8×2) at 520 °C; (d) (4×2)-$c$(8×2) at 580 °C; (e) (4×6) at 600 °C; (f) the "star burst" pattern revealing surface decomposition.